Behavioral and Brain Functions

RESEARCH

Open Access

Cofilin linked to GluN2B subunits of NMDA receptors is required for behavioral sensitization by changing the dendritic spines of neurons in the caudate and putamen after repeated nicotine exposure

Sunghyun Kim[1], Sumin Sohn[1] and Eun Sang Choe[1*]

Abstract

Background Nicotine dependence is associated with glutamatergic neurotransmission in the caudate and putamen (CPu) of the forebrain which includes alterations in the structure of dendritic spines at glutamate synapses. These changes after nicotine exposure can lead to the development of habitual behaviors such as smoking. The present study investigated the hypothesis that cofilin, an actin-binding protein that is linked to the GluN2B subunits of *N*-methyl-D-aspartate (NMDA) receptors regulates the morphology of dendritic spines in the neurons of the CPu after repeated exposure to nicotine.

Results Adult male rats received subcutaneous injections of nicotine (0.3 mg/kg/day) or vehicle for seven consecutive days. DiI staining was conducted to observe changes in dendritic spine morphology. Repeated subcutaneous injections of nicotine decreased the phosphorylation of cofilin while increasing the formation of thin spines and filopodia in the dendrites of medium spiny neurons (MSN) in the CPu of rats. Bilateral intra-CPu infusion of the cofilin inhibitor, cytochalasin D (12.5 μg/μL/side), restored the thin spines and filopodia from mushroom types after repeated exposure to nicotine. Similar results were obtained from the bilateral intra-CPu infusion of the selective GluN2B subunit antagonist, Ro 25-6981 (4 μM/μL/side). Bilateral intra-CPu infusion of cytochalasin D that interferes with the actin-cofilin interaction attenuated the repeated nicotine-induced increase in locomotor sensitization in rats.

Conclusions These findings suggest that active cofilin alters the structure of spine heads from mushroom to thin spine/filopodia by potentiating actin turnover, contributing to behavioral sensitization after nicotine exposure.

Keywords Striatum, Glutamate receptor, Nicotine dependence, Synaptic plasticity, Tobacco

*Correspondence:
Eun Sang Choe
eschoe@pusan.ac.kr
[1]Department of Biological Sciences, Pusan National University, 63-2 Busandaehak-ro, Geumjeong-gu, Busan 46241, Republic of Korea

Introduction

Nicotine, an addictive stimulant contained in tobacco products, remains a global concern due to its widespread use and associated health risks [1, 2]. Nicotine dependence is characterized by a compulsive and uncontrollable craving for nicotine, leading individuals to chronic tobacco use despite its harmful consequences [3]. Synaptic plasticity is a key factor in the development of nicotine dependence, which refers to the ability of a synapse to change by altering neurotransmission in response to stimuli, such as drug exposure [4, 5]. This phenomenon encompasses both electrophysiological and structural changes, serving as a driving force behind the development of drug dependence [6–8].

Nicotine binds to nicotinic acetylcholine receptors (nAChRs) in the caudate and putamen (CPu), a region primarily involved in habit formation such as tobacco smoking, leading to a cascade of events that results in the release of various neurotransmitters, including glutamate and dopamine [9–13]. These increases in neurotransmission lead to dendritic remodeling in the neurons of the CPu, which is characterized by increased dendritic spine density and development of habit learning [14–16]. Chronic exposure to nicotine and subsequent withdrawal induces long-lasting changes in synaptic structure, and the efficacy of neurons in the CPu, which is mediated primarily by stimulating the GluN2B subunits of *N*-methyl-D-aspartate (NMDA) receptors [15, 17]. Re-exposure to nicotine after six months of long-term withdrawal increases the density of the dendritic spines of neurons in the CPu [15]. These findings suggest that nicotine causes long-term changes in synaptic architecture in the neurons of the CPu by regulating the GluN2B subunits.

Morphological changes in the dendritic spines are tightly regulated by actin cycling, which is a complicated process directed by cofilin [18–20]. Cofilin is a member of the actin-depolymerization factor (ADF)/cofilin family, and depolymerizes actin structures, increasing actin turnover [21]. Therefore, an increase in the phosphorylation status of cofilin corresponds to an increase in its inactivation state, which is closely related to the development of drug dependence [22–24]. For instance, repeated exposure to cocaine increases the thin spines in the nucleus accumbens (NAc) by activating cofilin [22]. These findings suggest that changes in the phosphorylation status of cofilin are crucial for altering spine morphology in the NAc, which leads to drug dependence.

Nevertheless, several questions remain regarding how nicotine produces its dependence in the CPu that is related to changes in spine architecture despite being regulated by cofilin activity. Chronic exposure to drugs is closely related to the structural plasticity and simultaneous behavioral changes in rats. For instance, inhibition of actin cycling in the NAc contributes to increases in spine head diameter and density, and behavioral sensitization after challenge exposure to cocaine [25]. Therefore, this study determined the hypothesis that cofilin linked to the GluN2B subunits of the NMDA receptors is responsible for regulating the reorganization of the actin cytoskeleton in the dendritic spines of medium spiny neurons (MSN) of the CPu, which may contribute to nicotine-induced behavioral alterations.

Methods

Animals

Sprague–Dawley male rats (six weeks, 104 rats) were obtained from Hana Biotech (Gyeonggi-do, Korea). The rats were housed in pairs in a controlled environment with food and water provided *ad libitum*. They were housed in a 12 h light-dark cycle room (light on at 7 AM) at a temperature and humidity of 21–23 °C and 45–55%, respectively. The rats were allowed to acclimate for a week, and the experiment started when they weighed 250–310 g. The experiments were performed within the light cycle period. On the day of the experiment, injections were given to the rats in home cages to minimize stress.

Nicotine and drugs

Nicotine hydrogen tartrate salt was purchased from Sigma–Aldrich (St. Louis, MO, USA), dissolved in sterile 0.9% physiological saline (NaCl), and the pH was adjusted to 7.2–7.4 with sodium hydroxide (NaOH). Nicotine was administered subcutaneously (s.c.) in a 1 mL volume, and the nicotine concentration (0.3 mg/kg/day) was determined in previous studies [13]. The rats were randomly divided and were administered saline or nicotine for seven consecutive days. For acute nicotine, saline was administered (s.c.) for six consecutive days, and nicotine was then administered (s.c.) on the seventh day. All drugs, except nicotine, were purchased from Tocris Bioscience (Bristol, UK), and solutions were freshly prepared before use. The rats received the drugs through a bilateral intra-CPu infusion before the last exposure to saline or nicotine. Cytochalasin D (CytoD) inhibits the actin-cofilin interaction by binding to actin [26]. Thus, CytoD was used as a cofilin inhibitor. CytoD (12.5 μg/μL/side) was initially dissolved in the minimum concentration of dimethylsulfoxide (DMSO) and diluted in artificial cerebrospinal fluid (aCSF) containing (mM) 123 NaCl, 0.86 $CaCl_2$, 3.0 KCl, 0.89 $MgCl_2$, 0.50 NaH_2PO_4, and 0.25 Na_2HPO_4 aerated with 95% O_2/5% CO_2 (pH 7.2–7.4) or NaCl. Ro 25-6981 (4 μM/μL/side), a GluN2B-selective antagonist, was dissolved in phosphate-buffered saline (PBS). The same DMSO-aCSF solution and PBS were used as the vehicle controls. The concentrations of pharmacological drugs used in this study were determined from previous studies [27, 28].

Surgery and bilateral intra-CPu infusion of drugs

The rats were s.c. anesthetized with a mixture of Zoletil 50 (tiletamine and zolazepam, 75 μL/kg; Seoul, Virbac Korea) and Rompun (xylazine, 50 μL/kg; Seoul, Bayer Korea), then placed in a stereotaxic apparatus. Under aseptic conditions, a 23-gauge stainless steel double guide cannula (0.29 mm inner diameter, 13 mm in length) was implanted 1 mm anterior to the bregma, 2.5 mm left/right of the midline, and 5 mm below the surface of the skull. The guide cannula was sealed with a stainless-steel wire of the same length. The rats were then allowed seven days to recover from surgery before the experiment. On the day of the experiment, the inner steel wire was replaced with a 30-gauge stainless steel injection cannula (0.15 mm inner diameter, 13.5 mm in length) that protruded 0.5 mm from the guide cannula. Throughout the experiments, all drugs were infused bilaterally into the central part of the CPu 10 min before the final injection of saline or nicotine in a volume of 1 μL at a rate of 0.2 μL/min in freely moving rats. The progress of the injection was monitored by observing the movement of a small air bubble along the length of precalibrated PE-10 tubing inserted between the injection cannula and a 2.5 μL Hamilton microsyringe. After the infusion, the injector was left in place for an additional 5 min to reduce possible backflow along the injection tract. The physical accuracy of the injection was verified by reconstructing the microinjection placements.

Western blot analysis

Twenty rats were anesthetized with a mixture of Zoletil 50 and Rompun and decapitated 1 h after the final exposure to saline or nicotine. The brains were removed, frozen in isopentane at −70℃, and stored in a deep freezer until use. Brain slices were cut serially using a cryostat (Leica, Nussloch, Germany) at −20℃, after which both sides of CPu were removed using a steel borer (3 mm inner diameter). All tissue samples were sonicated three times for 9 s in a lysis buffer containing (mM) 10 Tris-HCl (pH 7.4), 5 NaF, 1 Na_3VO_4, 1 EDTA, and 1 EGTA. The lysates were incubated on ice for 1 h and centrifuged twice at 13,200 rpm for 30 min at 4℃. The supernatants were used in the experiment. The concentrations of solubilized proteins in the supernatants were determined using a Bio-Rad Protein Assay (Bio-Rad Laboratories, Hercules, CA, USA) according to the Bradford method. The proteins were resolved by 10–12% sodium dodecyl sulfate (SDS)-polyacrylamide gel electrophoresis and transferred to nitrocellulose membranes. The membranes were blocked with 5% skim milk in tris-buffered saline and tween-20 (TBST) for 1 h at room temperature (RT). The membranes were then washed three times with TBST and probed with anti-phospho-cofilin and LIMK1/2 (Cat.# 3311 and 3841; rabbit polyclonal; 1:1,000; Cell Signaling Technology, Danvers, MA, USA) or anti-GAPDH (Cat.# 60004-1-Ig; mouse monoclonal; 1:20,000; Proteintech, Chicago, IL, USA) overnight at 4 ℃ on a shaker. The antibodies were diluted with 2% skim milk in TBST. After three washes, the membranes were incubated with HRP-labeled goat anti-rabbit secondary antiserum (1:10,000; KPL, Gaithersburg, MD, USA) or anti-mouse secondary antiserum (polyclonal, 1:10,000; Proteintech) for 1 h at RT. The images were taken on an iBright CL1000 (Thermo Fisher Scientific, Waltham, MA, USA) using enhanced chemiluminescence reagents (Ab Frontier, Seoul, South Korea). The membranes were then immersed in stripping buffer containing 50 mM Tris-HCl (pH 7.0), with 2% SDS and 50 mM dithiothreitol (DTT) for 1 h at 70℃. The stripped membranes were re-probed with anti-cofilin (Cat.# 5175; rabbit monoclonal; 1:2,000; Cell Signaling Technology) and anti-LIMK1 (Cat.# 3842; rabbit polyclonal; 1:2,000; Cell Signaling Technology) antibodies. Immunoreactive images of protein bands using the CL1000 were semi-quantified by counting the number of pixels using NIH Image 1.62 software.

Immunofluorescence analysis

Eight rats were perfused transcardially with ice-cold 4% paraformaldehyde (PFA) for 7 min following anesthesia administered 1 h after the final exposure to saline or nicotine. The brains were then removed and post-fixed in a 4% PFA/10% sucrose for 2 h at 4℃, followed by PBS (pH 7.2)/20% sucrose overnight at 4℃ [29]. For tissue preparation, 30-μm-thick coronal slices from the CPu were prepared from saline or nicotine-treated rats using a VT1000S vibratome (Leica). Three slices per rat, +0.8 to +1.2 mm away from the bregma, were prepared for staining. The slices were blocked with a blocking solution containing 0.3% Triton X-100, 5% normal goat serum, and 0.1% bovine serum albumin (BSA) in PBS (pH 7.4) for 2 h at RT. The slices were washed three times with 0.3% Triton X-100 in PBS and incubated with the primary antibody, anti-phospho-cofilin (1:500) overnight at 4 ℃. The antibodies were diluted in PBS containing 0.1% BSA and 0.3% Triton X-100. The slices were then incubated in a mixture of secondary antibodies containing goat anti-rabbit Alexa Fluor 488 (Cat.# ab150077; polyclonal; 1:1,000; Abcam, Cambridge, MA, USA) for 2 h at RT. After three washes, the slices were mounted with an aqueous mounting medium (Abcam). Alexa Fluor 594 anti-DARPP-32 antibody (Cat.# ab214852; rabbit monoclonal; 1:100; Abcam) was used to identify MSN. The images were taken using a confocal microscope (LSM 800, Carl Zeiss, Jena, Germany) equipped with a 40×/1.2 NA water-immersion objective lens. The number of neurons and co-localized puncta that co-express phospho-cofilin and DARPP-32 in the CPu was analyzed using a cell counter and the image calculator function in ImageJ/

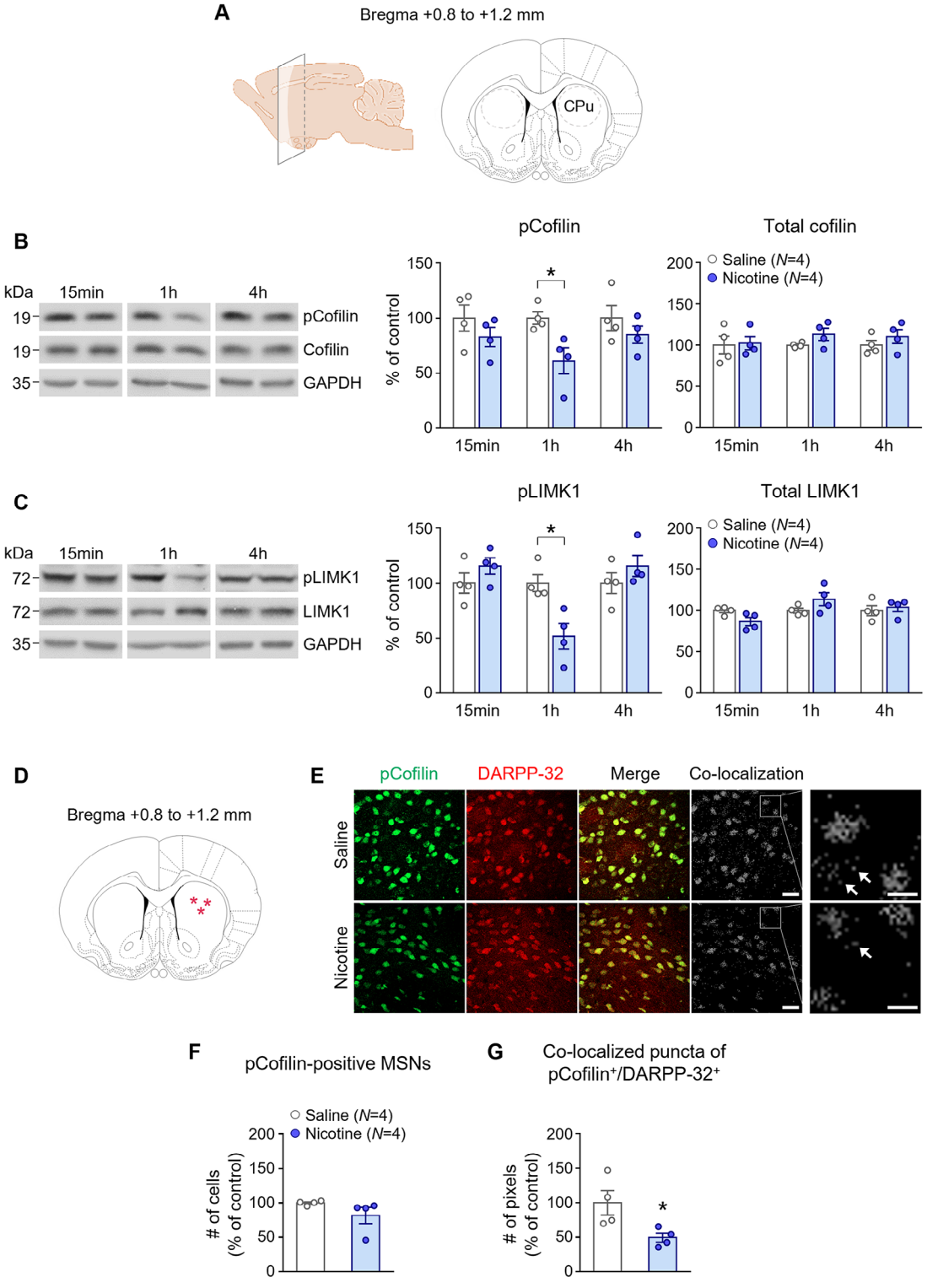

Fig. 1 Nicotine decreases pCofilin- and pLIMK1 levels in the CPu. (**A**) Areas of the CPu punched out for conducting western blot analysis within anterior to posterior (AP) coordinates of + 1.2 to + 0.8 mm. (**B**, **C**) Repeated nicotine exposure decreased pCofilin- and pLIMK1-IR at the 1 h time point. (**D**) A brain section for conducting immunofluorescence staining within the AP coordinates of + 1.2 to + 0.8 mm. The red stars in the CPu indicate the areas captured in photomicrographs shown in Figure E. (**E**) Repeated nicotine exposure decreased pCofilin-IR in MSN of the CPu. The scale bar represents 30 μm. The arrows in the magnified images indicate puncta. The scale bar represents 10 μm. (**F**, **G**) Quantitative analysis showed that repeated nicotine exposure decreased the number of co-localized puncta of pCofilin- and DARPP-32-IR but not the number of pCofilin-positive neurons in the CPu. $N = 4$ rats per group. *$p < 0.05$

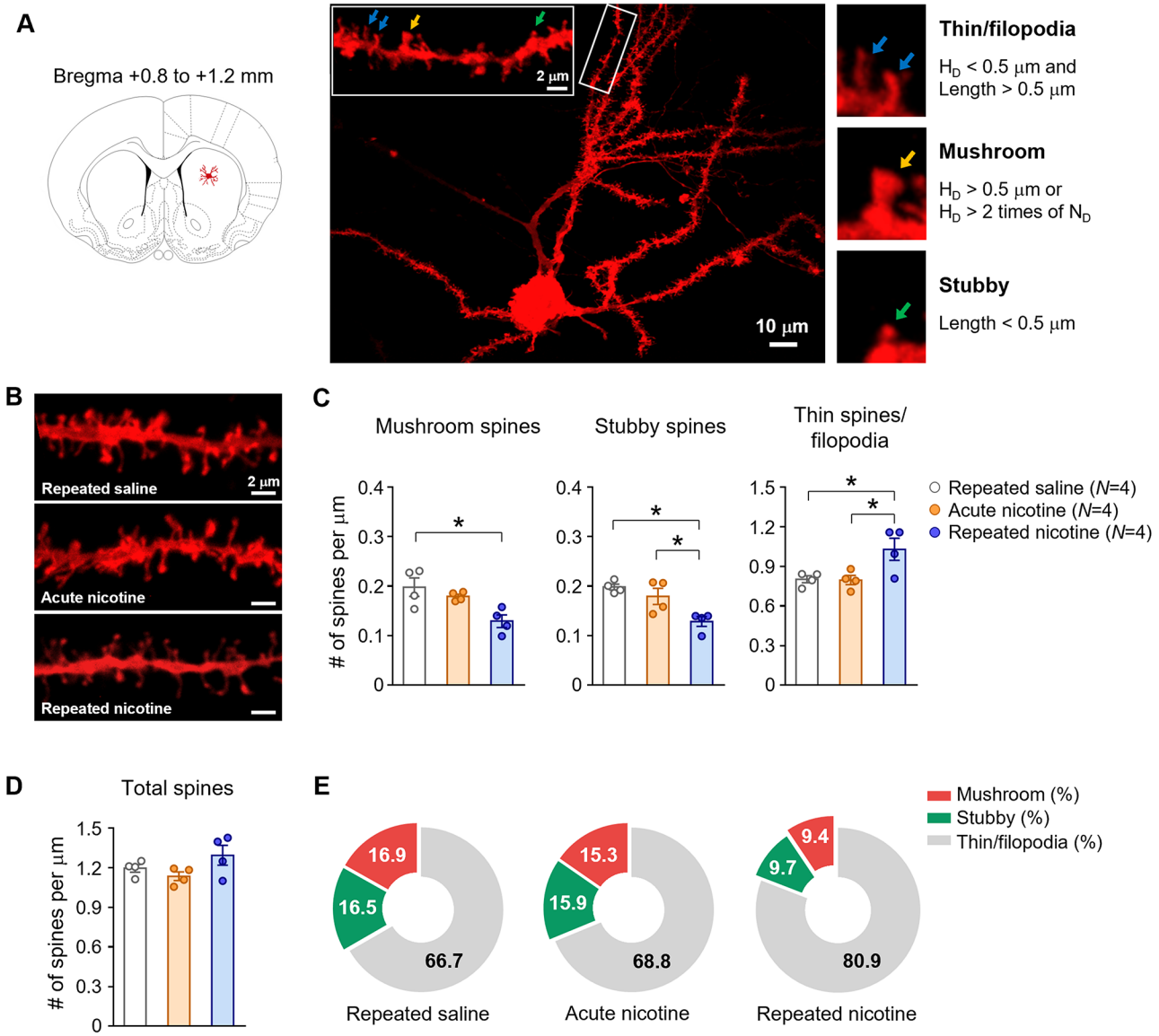

Fig. 2 Nicotine alters dendritic spine morphology in the MSN. (**A**) DiI staining of MSN in the CPu and three types of dendritic spines: From the top right, thin spines/filopodia (blue arrows), a mushroom spine (yellow arrow), and a stubby spine (green arrow). (**B**, **C**) Repeated, not acute, nicotine exposure decreased the number of mushroom/stubby spines, while it increased thin spines/filopodia. (**D**) Neither repeated nor acute nicotine exposure affected the density of the spines. (**E**) Distribution of dendritic spines in each group. $n = 1780$ (Repeated saline), 1819 (Acute nicotine) and 1959 (Repeated nicotine) spines. $N = 4$ rats per group. $^*p < 0.05$

Fiji software (NIH, USA) and Zen Blue software 3.4 (Carl Zeiss) [30].

DiI staining

The dendritic spines were visualized by staining the MSN of the CPu with a lipophilic carbocyanine dye DiI (Invitrogen, Carlsbad, CA), which is used widely for neuronal tracing in fixed tissues [31, 32]. DiI staining was performed as described elsewhere [32]. Briefly, forty-four rats were perfused transcardially with ice-cold 1.5% PFA for 15 min following anesthesia 1 h after the final exposure to saline or nicotine. The brains were removed and post-fixed in a 4% PFA for 2 h at 4℃. Coronal slices, 150 μm in thickness, were then prepared using the VT1000S vibratome. The slices were mounted onto glass slides circled with a solvent-resistant histology pen, and powdered DiI was applied to the slices using a sharp glass tip. The inside of the circle was then filled with PBS (pH 7.4) to prevent the tissue from drying out during staining. DiI was allowed to diffuse into the slices for 24 h at 4℃, and labeled slices were washed lightly with PBS and fixed in 4% PFA for 1 h at RT. The slices were washed three times and mounted in an antifade aqueous medium (Vector Laboratories, Burlingame, CA).

Confocal imaging and spine analysis

DiI-labeled slices were imaged using a Zeiss LSM 800 confocal microscope. Neurons filled with DiI were visualized with the 40×/1.2 NA water-immersion objective lens at a 1.5× optical zoom. The images were captured at a 16-bit image depth and stored at a resolution of 2048×2048 pixels (pixel scale 0.05×0.05 μm; field size 106.48×106.48 μm). Neurons were scanned at intervals of 0.75 to 0.8 μm along the z-axis, with the number of z-stack planes determined by individual dendritic segments. Z-stack images were merged using orthogonal projection in the Zen Blue software. Dendrites containing dendritic spines, each 20 μm in length, were selected for the analysis. Five dendrites per neuron and approximately five neurons per animal were analyzed. Spine analyses were performed manually using established criteria (Fig. 2A) [33, 34], categorizing the spines into three distinct types: (i) mushroom-like spines characterized by a head diameter > 0.5 μm or greater than two times the spine neck diameter; (ii) stubby spines defined as dendritic protrusions with no discernable head enlargement and a length of ≤ 0.5 μm; (iii) thin/filopodia-like spines that are dendritic protrusions with a length of > 0.5 μm and a head diameter < 0.5 μm or no discernable head enlargement.

Crosslinking assays for surface receptors

The surface expression of GluN2B subunits was measured by performing an assay using a bis(sulfosuccinimidyl) suberate (BS^3) crosslinking reagent that is membrane-impermeable and covalently crosslinks with surface-expressed receptors [35]. Eight rats were decapitated 1 h after the final exposure to saline or nicotine following anesthesia. Both sides of the CPu were dissected on a chilled brain matrix with a steel borer (3 mm inner diameter). Chopped tissue samples were added to 1.5 ml tubes containing ice-cold aCSF. Subsequently, 52 mM of BS^3 (Thermo Fisher Scientific) was added immediately, and the samples were incubated with gentle agitation for 30 min at 4℃. The crosslinking reaction was quenched by adding 1 M glycine with gentle agitation for 10 min at 4℃. The samples were then spun down, and the supernatants were removed. A lysis buffer containing (mM) 25 HEPES, 500 NaCl, 2 EDTA, 1 DTT, 1 PMSF, 20 NaF, 1 Na_3VO_4, 0.1% NP-40, and protease/phosphatase inhibitor cocktail (Thermo Fisher Scientific) was added to the pellets, which were then sonicated for 5 s on ice. The lysates were centrifuged and analyzed directly by SDS-PAGE with 4–15% gradient gels (Bio-Rad Laboratories). The gels were transferred into nitrocellulose membranes that were incubated with antiserum against GluN2B (Cat.# 14544; rabbit monoclonal; 1:1,000; Cell Signaling Technology). After incubation in HRP-labeled goat anti-rabbit secondary antiserum (1:10,000; KPL), the membranes were developed using Westsave UP (Ab Frontier). For normalization of the samples, β-actin (Cat.# 4970; rabbit monoclonal; 1:10,000; Cell Signaling Technology) was used as a loading control. The immunoreactive protein bands imaged using the CL1000 were semi-quantified by counting the number of pixels using NIH Image 1.62 software.

Behavioral assessments

Behavioral assessments were conducted as described previously [12, 36]. Twenty-four rats received a bilateral intra-CPu infusion of CytoD before the final injection of saline or nicotine. After drug infusion, the locomotor activity was measured in an open field using an infrared photocell-based Opto-Varimex-4 Auto-Track (Columbus Instruments, Columbus, OH, USA) under sound-attenuated and illuminated conditions. The rats were placed in a standard transparent rectangular chamber (44.5 cm × 44.5 cm × 24 cm) and habituated for 30 min before the experiment to avoid environmental variations. Three pairs of sensors were positioned on the orthogonal axes in the cage to provide the coordinates of rat movements in the locomotor testing chamber. Each pair of sensors produced 16 infrared light beams intersecting the animal cage (beam scan rate = 10 Hz). This Auto-Track system sensed the presence of animals using data generated by infrared beam blocking. The locomotor activities were recorded for over 90 min after a daily injection of saline or nicotine. The measurements were transferred to a computer using Opto-Varimex-4 Auto-Track Rapid Release software (v4.99B software, Columbus Instruments). All rats were anesthetized with a mixture of Zoletil 50 and Rompun, and the brains were removed to identify the placements of the guide cannulae.

Statistical analysis

Statistical analysis was conducted using GraphPad Prism 6 software (GraphPad Software Incorporation, San Diego, CA, USA). The results are presented as means ± standard errors. The statistical significance was determined for p-values < 0.05. The differences between groups in terms of the number of immunoreactive pixels per measured area, as determined by western blotting, immunofluorescence, and crosslinking assay, were assessed using an unpaired t-test or two-way analysis of variance (ANOVA) followed by a Tukey's multiple comparisons test. For DiI-stained dendritic spine analysis, statistical significance was determined using either one- or two-way ANOVA followed by a Tukey's multiple comparisons test. Chi-square test was used to determine whether the differences in proportions between groups in the donut charts were statistically significant. The statistical significance of the differences in the total distance traveled between groups was determined by repeated

measures (RM) two-way ANOVA followed by a Tukey's multiple comparisons test. Power analysis was conducted using RStudio (version 2023.12.0; Posit, Boston, MA, USA) to ensure sufficient statistical power, and a power level greater than 0.8 ($p>0.8$) was achieved throughout the experiments.

For statistical analysis of changing the morphology of dendritic spines, the following procedure was used [37]. Measurements from individual dendritic segments were averaged within each neuron to obtain a cell-based value. Then, the values were averaged across neurons in each rat to derive rat-based values. Finally, independent rat-based values were averaged across all rats in the experimental groups to produce group-based statistical values.

Results

Repeated exposure to nicotine decreases phosphorylated (p)cofilin immunoreactivity (IR) in the MSN of the CPu

The first set of experiments examined whether repeated exposure to nicotine alters the cofilin activity in the MSN of the CPu in rats (Fig. 1A). Repeated nicotine exposure decreased the pCofilin-IR compared to the repeated saline group 1 h after the final injection of saline or nicotine (Fig. 1B: time effect, $F(2, 12)=0.7053$, $p=0.5133$; nicotine effect, $F(1, 6)=18.30$, $p=0.0052$, two-way ANOVA). On the other hand, this decrease was restored at the 4 h time point. Similarly, repeated nicotine exposure decreased the IR of pLIMK1 that phosphorylates cofilin in neural tissues [38] 1 h after the final injection of nicotine (Fig. 1C: time effect, $F(2, 12)=10.59$, $p=0.0022$; nicotine effect, $F(1, 6)=0.3753$, $p=0.5626$, two-way ANOVA). This decrease was restored at the 4 h time point. Repeated nicotine exposure did not affect total cofilin- and LIMK1-IR in the CPu at any time point examined (Fig. 1B, C). We examined the changes in pCofilin-IR in the MSN of the CPu because more than 97% of neurons in the CPu are identified as MSN [39]. Repeated nicotine exposure did not change the number of neurons that displayed both pCofilin- and the marker for GABAergic MSN, DARPP-32-IR, in the CPu (Fig. 1D–F). However, the co-localized puncta of pCofilin and DARPP-32 decreased within the cell bodies and neuropils after repeated nicotine exposure (Fig. 1E, G: 1G, $t(6)=2.652$, $p=0.0379$, unpaired t-test).

Repeated exposure to nicotine induces the remodeling of dendritic spines

Since repeated nicotine exposure activated cofilin by decreasing the level of pCofilin, the following experiments investigated whether repeated nicotine exposure induces morphological changes in the dendritic spines of MSN. Since cofilin activity within 1 h after repeated administration of nicotine was altered, changes in the shape of dendritic spines were analyzed during the same time period. The neurons were labeled with DiI, a lipophilic membrane staining reagent that produces a fluorescent signal for neuronal labeling (Fig. 2A). The dendritic spines were captured and categorized according to their shapes as mushroom, stubby, and thin/filopodia [40]. The number of mushroom ($F(2, 9)=7.113$, $p=0.0140$, one-way ANOVA) and stubby ($F(2, 9)=9.633$, $p=0.0058$, one-way ANOVA) spines decreased 1 h after repeated nicotine exposure compared to the saline-treated group (Fig. 2B, C), while the number of thin spines/filopodia spines increased (Fig. 2B, C: 2 C, $F(2, 9)=5.963$, $p=0.0224$, one-way ANOVA). However, the total number of dendritic spines did not change after repeated exposure to nicotine (Fig. 2D). We calculated the relative enrichment of the three types of spines by normalizing them to the total number of spines in each group to evaluate these changes comprehensively throughout the experiments. The proportion of mushroom and stubby spines among all spines decreased from 16.9 to 9.4% and 16.5–9.7%, respectively, after repeated exposure to nicotine (Fig. 2E). In contrast, repeated nicotine exposure increased the ratio of thin spines/filopodia among the total spines from 66.7 to 80.9% (Fig. 2E: repeated saline vs. repeated nicotine, $\chi^2 = 97.77$, $df=2$, $p<0.0001$, chi-square test; acute nicotine vs. repeated nicotine, $\chi^2 = 73.53$, $df=2$, $p<0.0001$, chi-square test). We also performed an additional experiment by adding an acute nicotine group to determine short-term effects of nicotine on spine morphology. The results showed that administration of acute nicotine did not alter the structure and number of dendritic spines (Fig. 2B–E).

Inhibition of cofilin restores the nicotine-induced remodeling of dendritic spines

This study determined the contribution of cofilin to the remodeling of dendritic spines after repeated nicotine exposure. The cofilin inhibitor, CytoD, which interferes with the actin-cofilin interaction, was used [26]. Reconstruction of microinjection placements showed that the majority of the bilateral intra-CPu infusion of CytoD was confined to the center of the CPu within the AP coordinates of +1.2 to +0.8 mm (Fig. 3A). The bilateral intra-CPu infusion of CytoD (12.5 μg/μL/side) restored the repeated nicotine-induced decrease in the number of mushroom spines (Fig. 3B, C: drug effect, $F(1, 12)=2.170$, $p=0.1665$; nicotine effect, $F(1, 12)=18.20$, $p=0.0011$, two-way ANOVA), while it decreased the number of thin spines/filopodia (Fig. 3B, C: drug effect, $F(1, 12)=11.68$, $p=0.0051$; nicotine effect, $F(1, 12)=4.527$, $p=0.0548$, two-way ANOVA). The infusion of CytoD did not alter the number of stubby spines (Fig. 3B, C). No significant difference in the total number of dendritic spines was observed after the infusion of CytoD (Fig. 3D). The infusion of CytoD restored the proportion of mushroom spines among all spines from 9.3 to 13.7% and that of

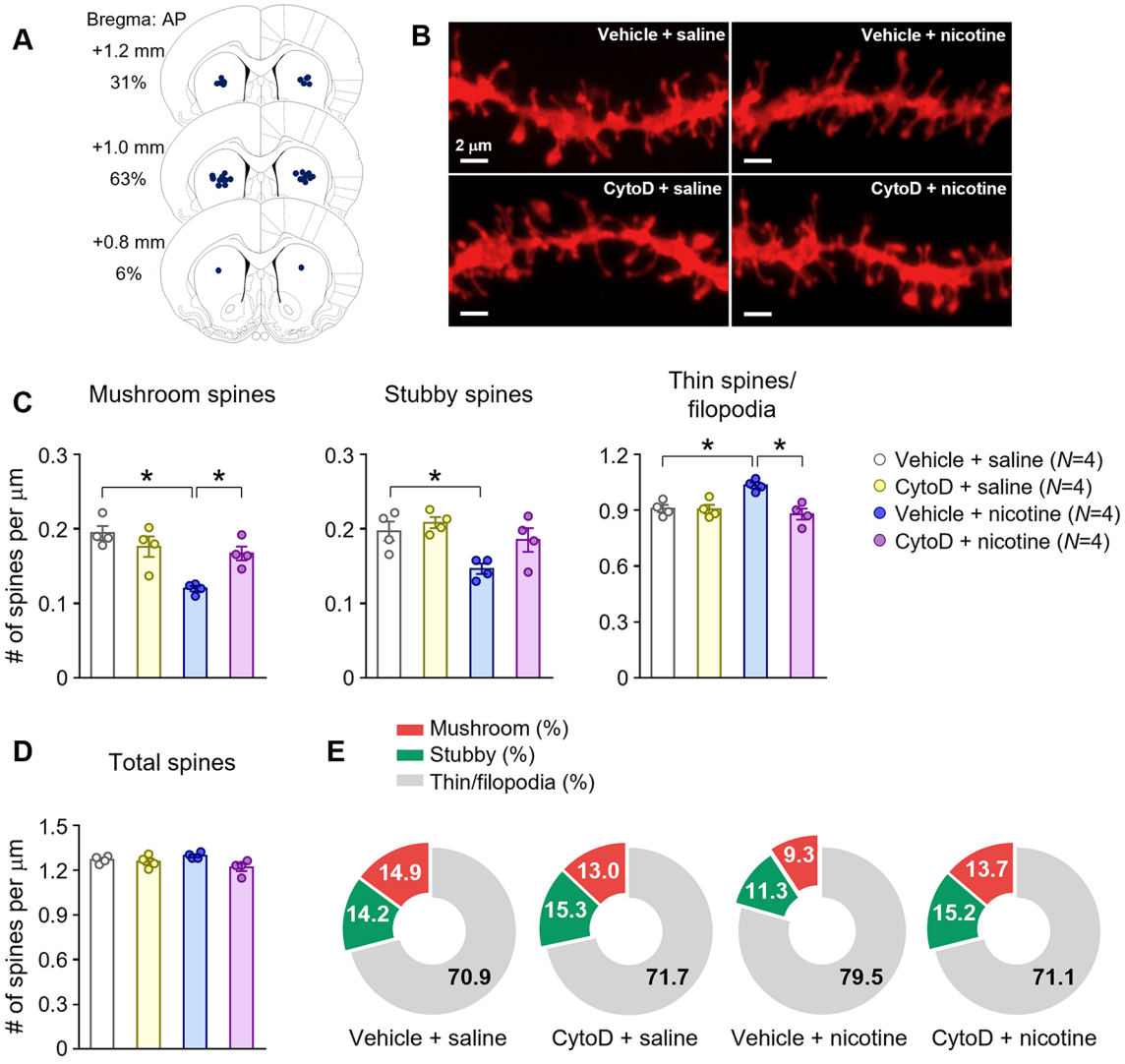

Fig. 3 Inhibition of cofilin restores the nicotine-induced change in dendritic spine morphology. (**A**) Bilateral intra-CPu infusion of cytochalasin D (CytoD) was confirmed by reconstructing the microinjection placements. (**B**, **C**) Inhibition of cofilin by CytoD restored the changes in mushroom spines and thin spines/filopodia after repeated nicotine exposure. (**D**) Inhibition of cofilin did not affect the density of the spine. (**E**) Distribution of dendritic spines in each group. $n = 3183$ (Vehicle + saline), 2793 (CytoD + saline), 2594 (Vehicle + nicotine) and 2413 (CytoD + nicotine) spines. $N = 4$ rats per group. *$p < 0.05$

thin spines/filopodia from 79.5 to 71.1%, which was similar to the saline control groups (Fig. 3E: vehicle saline vs. vehicle nicotine, $\chi^2 = 74.20$, $df = 2$, $p < 0.0001$, chi-square test; vehicle nicotine vs. CytoD nicotine, $\chi^2 = 48.02$, $df = 2$, $p < 0.0001$, chi-square test).

Membrane expression of the GluN2B subunits regulates the nicotine-induced remodeling of dendritic spines

This experiment investigated the linking of GluN2B subunits in the cofilin-induced synaptic remodeling in the rat CPu after repeated exposure to nicotine. In a BS^3 cross-linking assay, repeated nicotine exposure increased the surface and intracellular expression of the GluN2B subunits (Fig. 4A: surface, $t(6) = 3.900$, $p = 0.0080$; intracellular, $t(6) = 3.769$, $p = 0.0093$, unpaired t-test). A bilateral intra-CPu infusion of the GluN2B-selective antagonist, Ro 25-6981 (4 μM/μL/side) increased the repeated nicotine-induced decrease in pCofilin-IR (Fig. 4C: drug effect, $F(1, 8) = 17.17$, $p = 0.0032$; nicotine effect, $F(1, 8) = 4.031$, $p = 0.0796$, two-way ANOVA). The physical accuracy of bilateral intra-CPu infusion of Ro 25-6981 was confirmed by reconstructing microinjection placements within the AP coordinates of +1.2 to +0.8 mm (Figs. 4B and 5A). Bilateral intra-CPu infusion of Ro 25-6981 restored the repeated nicotine-induced decrease in the number of mushroom spines (Fig. 5B, C: drug effect, $F(1, 12) = 71.30$, $p < 0.0001$; nicotine effect, $F(1, 12) = 29.82$, $p = 0.0001$, two-way ANOVA), while it restored the repeated nicotine-induced increase in the number of thin spines/filopodia (Fig. 5B, C: drug effect, $F(1, 12) = 62.26$, $p < 0.0001$;

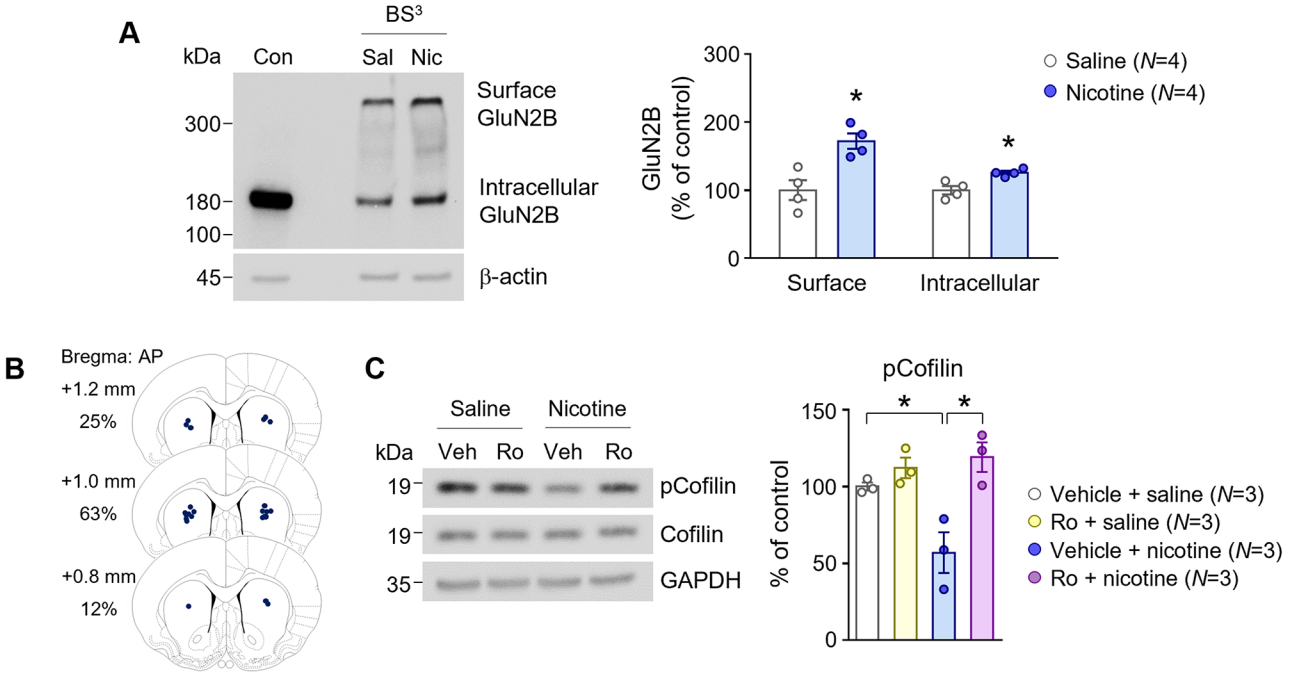

Fig. 4 Blockade of GluN2B subunits restores the nicotine-induced increase in cofilin activity. (**A**) Repeated nicotine exposure increased the expression of both surface- and intracellular GluN2B subunits. $N=4$ rats per group. (**B**) Bilateral intra-CPu infusion of the GluN2B subunit antagonist, Ro 25-6981 (Ro), was confirmed by reconstructing microinjection placements. (**C**) Blockade of the GluN2B subunits with Ro elevated the repeated nicotine-induced decrease in pCofilin-IR. $N=3$ rats per group. *$p<0.05$

nicotine effect, $F(1, 12)=70.03$, $p<0.0001$, two-way ANOVA). However, blockade of GluN2B subunits by infusing Ro 25-6981 did not affect stubby spines (Fig. 5B, C). There was no difference in the total number of dendritic spines after blocking the subunits (Fig. 5D). The infusion of Ro 25-6981 restored the proportion of mushroom spines and thin spines/filopodia among all spines from 7.1 to 20.5% and 79.9–62.2%, respectively, which was similar to the saline control groups (Fig. 5E: vehicle saline vs. vehicle nicotine, $\chi^2 = 212.4$, $df=2$, $p<0.0001$, chi-square test; vehicle nicotine vs. Ro 25-6981 nicotine, $\chi^2 = 239.4$, $df=2$, $p<0.0001$, chi-square test).

Inhibition of cofilin regulates the nicotine-induced behavioral sensitization in rats

This study determined the contribution of cofilin-induced synaptic remodeling in the rat CPu to changes in behavioral sensitization after repeated nicotine exposure (Fig. 6A). Since cofilin activation is linked to the increase in the expression of GluN2B subunits after repeated exposure to nicotine, involvement of actin-cofilin interaction in regulating locomotor sensitization was determined. A reconstruction of microinjection placements showed that the majority of the bilateral intra-CPu infusion of CytoD was confined to the center of the CPu (Fig. 6B). The bilateral intra-CPu infusion of CytoD (12.5 μg/μL/side), prior to the final injection of nicotine decreased the repeated nicotine-induced increase in total distance travelled over 90 min (Fig. 6C: time effect, $F(6, 120)=8.565$, $p<0.0001$; drug effect, $F(3, 20)=23.04$, $p<0.0001$, RM two-way ANOVA). On the last day of nicotine injection, CytoD decreased the duration of the effects of nicotine on the locomotor activity (Fig. 6D: time effect, $F(20, 400)=25.09$, $p<0.0001$; drug effect, $F(3,20)=10.87$, $p=0.0002$, RM two-way ANOVA). However, the bilateral intra-CPu infusion of CytoD did not affect the total distance traveled following repeated exposure to saline (Fig. 6C, D).

Discussion

The present study shows that changes in cofilin activity by stimulating the GluN2B subunits of the NMDA receptors are necessary for remodeling the dendritic spines in the MSN of the CPu and simultaneous behavioral sensitization after chronic nicotine exposure in rats. Repeated, but not acute, nicotine exposure induces shrinkage of the spine heads, which is characterized by changes in the types of spines from mushroom to thin spines/filopodia.

Cofilin induces the disassembly and reorganization of F-actin through its severing activity, playing a pivotal role in promoting actin turnover and shaping spine morphology [19, 41, 42]. In the present study, repeated nicotine exposure reduces cofilin phosphorylation, resulting in the activation of cofilin. The inhibition of cofilin activity by disrupting the actin-cofilin interaction restores the cofilin-dependent shrinkage of spine heads. Similar

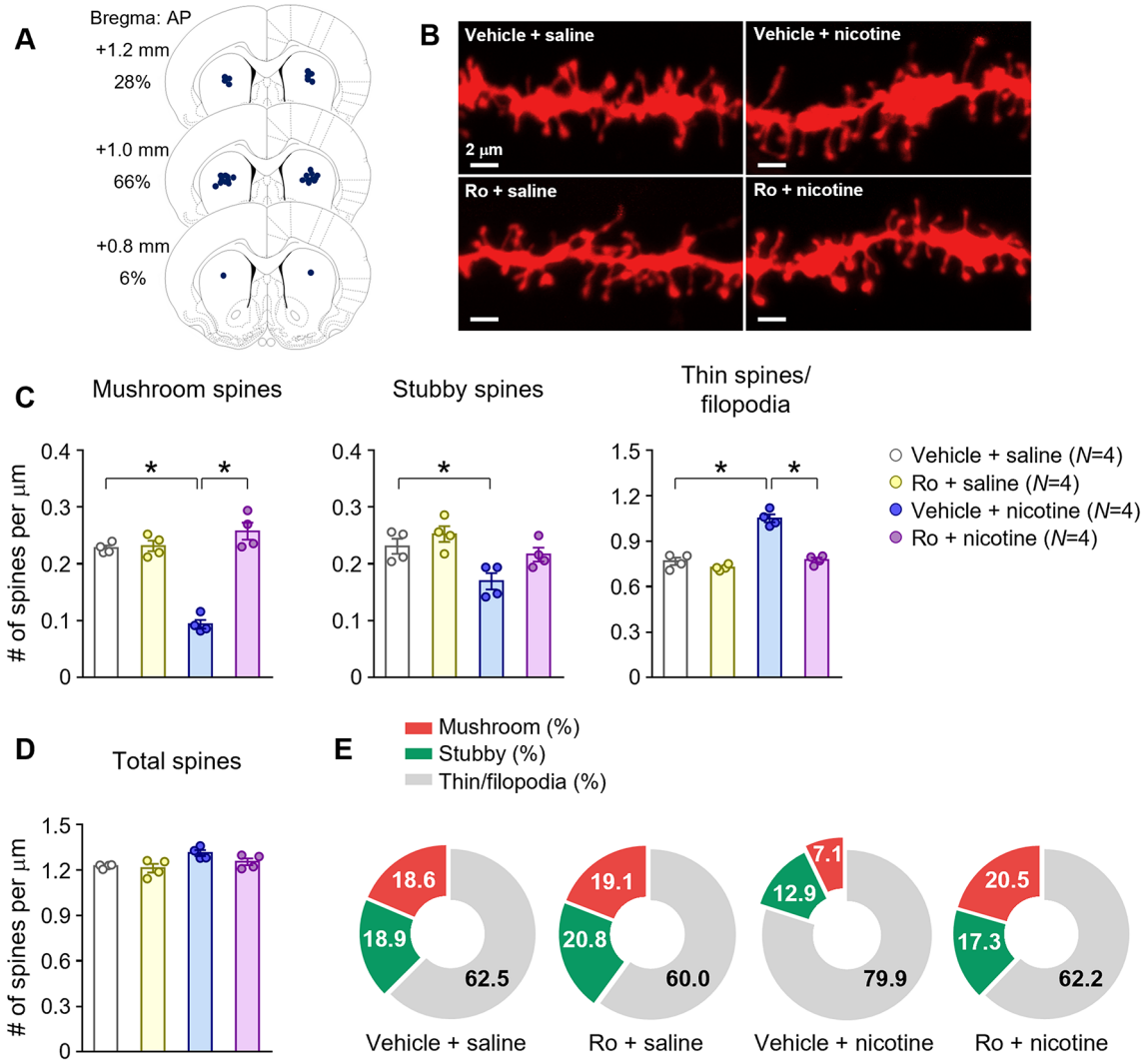

Fig. 5 Blockade of GluN2B restores the nicotine-induced change in dendritic spine morphology. (**A**) Bilateral intra-CPu infusion of Ro was confirmed by reconstructing the microinjection placements. (**B**, **C**) Blockade of GluN2B subunits with Ro restored the changes in mushroom spines and thin spines/filopodia induced by repeated nicotine exposure. The scale bar represents 2 μm. (**D**) Blockade of the GluN2B subunits did not affect the density of the spines. (**E**) Distribution of dendritic spines in each group. $n = 2450$ (Vehicle + saline), 2424 (Ro + saline), 2623 (Vehicle + nicotine) and 2509 (Ro + nicotine) spines. $N = 4$ rats per group. $^{*}p < 0.05$

finding has been reported by a previous study investigating the cofilin-mediated increase in thin spines in the NAc after repeated cocaine exposure [22]. However, inhibition of cofilin activity does not affect the morphological changes to the stubby spines induced by repeated nicotine exposure. These findings suggest that the actin-cofilin interaction leads to the shrinkage of spines from mushroom-shaped to thin spines/filopodia by depolymerizing branch structures in the spine heads. Therefore, it can be inferred that cofilin is responsible for changes in the morphology of dendritic spines by altering branch formation and the diameter of the spine heads in the MSN of the CPu.

Parallel to these findings, repeated nicotine exposure decreases the phosphorylation of LIMK1, an upstream regulator of cofilin in the CPu. Previous studies have demonstrated that LIMK1 is the direct upstream regulator of the actin-depolymerizing activity of cofilin in vitro and in vivo [43–45]. Furthermore, the severing activity of cofilin through LIMK1 contributes to changes in the synaptic structure and behaviors in response to cocaine exposure [22, 46, 47]. For instance, reinstatement of cocaine-seeking behavior is potentiated when actin cycling is disrupted by either upregulating actin depolymerization by inhibiting LIMK1 or polymerizing actin [46]. The inhibition of cofilin activity attenuates the repeated nicotine-induced increase in behavioral sensitization in rats in the present study. Taken together, these findings suggest that the activation of cofilin directed by LIMK1 in response to repeated nicotine enhances actin

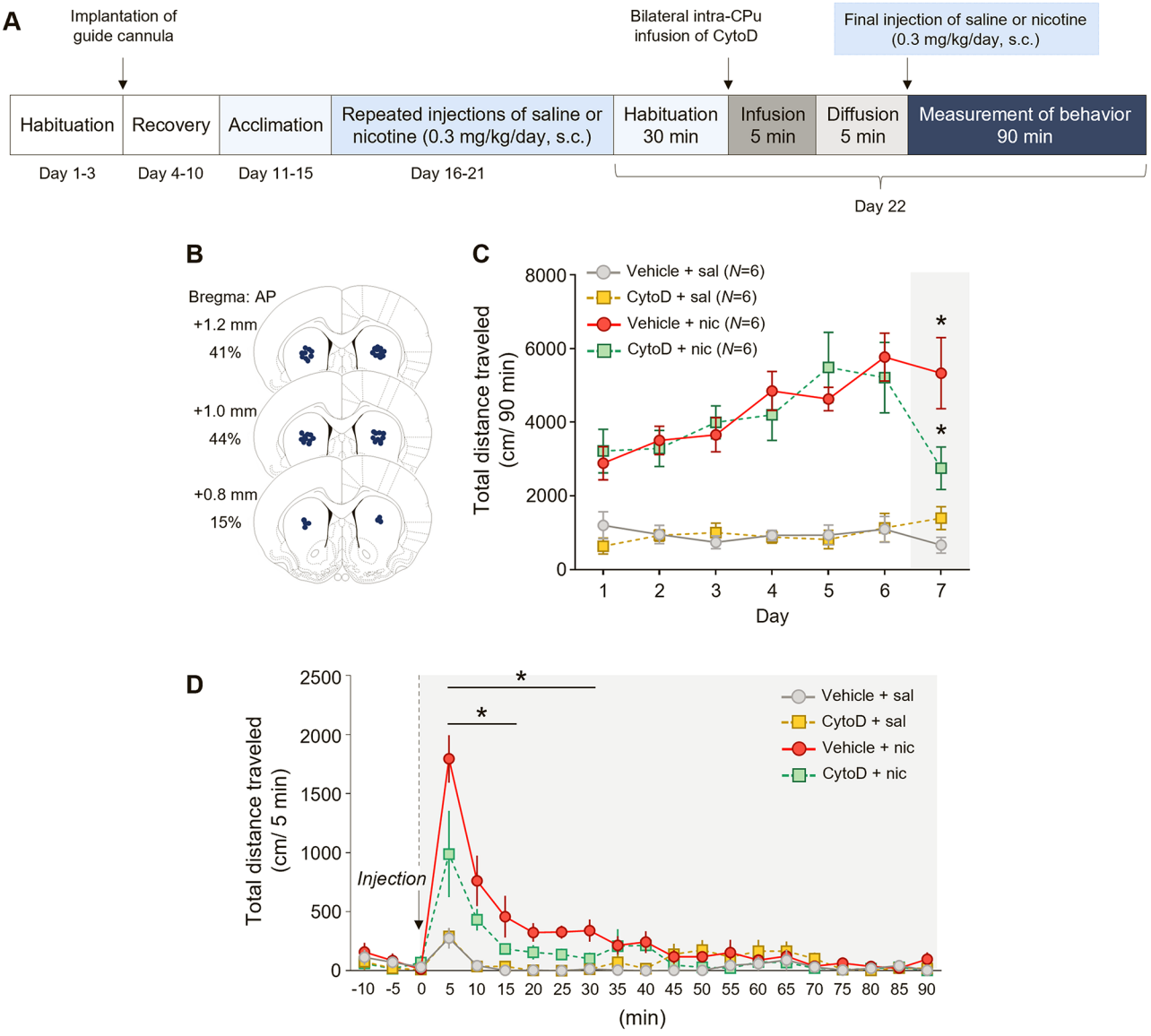

Fig. 6 Inhibition of cofilin decreases the nicotine-induced behavioral sensitization. (**A**) Timeline. (**B**) Intra-CPu infusion of the CytoD was confirmed by reconstructing microinjection placements. (**C**, **D**) Bilateral intra-CPu infusion of CytoD decreased the repeated nicotine-induced increase in locomotor activity in rats. $N = 6$ rats per group. $^{*}p < 0.05$

turnover, which leads to nicotine dependence via changes in the spine morphology.

Dendritic spines are small protrusions in the dendrites of neurons, which form the postsynaptic component of most excitatory synapses in the brain. The present study monitored the changes in the secondary and tertiary dendrites of MSN that lead to cellular and behavioral changes after psychostimulants exposure [32, 40, 48, 49]. The changes in morphology and the density of spines induce synaptic remodeling in the NAc and prefrontal cortex after nicotine or cocaine exposure [40, 50–52]. In the present study, however, repeated nicotine exposure does not affect the density and total number of dendritic spines. Instead, it alters the proportion of each spine type only. Approximately 80% of the total spines were thin spines/filopodia, while approximately 9% were mushroom spines in response to repeated exposure to nicotine. The distal branches, such as the fifth- and sixth-order branches or beyond, could provide the effect of repeated nicotine on changes in the density and morphology of spines [48, 53]. While this study employs the traditional classification of spines into distinct types–mushroom, stubby, and thin/filopodia–it is essential to recognize that spine morphology exists as a continuum rather than fitting neatly into discrete categories [54–56]. Considering this continuum-based perspective, the distinctions between spine types in the present study may represent momentary changes in the synaptic adaptation

process in response to nicotine exposure. Therefore, cofilin seems to upregulate synaptic plasticity by changing the shape of the spine heads rather than the density of spines in the MSN of the CPu after repeated exposure to nicotine.

The present study further demonstrates that stimulation of the GluN2B subunits integrates changes in the morphology of the dendritic spines of MSN by upregulating the cofilin activity in response to nicotine exposure. Repeated nicotine exposure increases the overall expression of the GluN2B subunits in the CPu, particularly on the membrane surface. Consistent with the present findings, previous studies have demonstrated a correlation between synaptic GluN2B subunits and alterations in spine morphology of striatal neurons following exposure to cocaine or nicotine [40, 52, 57, 58]. Rats in early withdrawal from cocaine self-administration increase excitatory inward ion currents that are mediated by stimulating the GluN2B subunits [33]. In addition, chronic nicotine exposure has been shown to elevate ion conductance from the GluN2B subunits in the CPu [17]. In this study, blockade of the GluN2B subunits restores the repeated nicotine-induced increase in cofilin activity by decreasing its phosphorylation, suggesting that the subunits are likely coupled to form thin spines/filopodia instead of mushroom spines. Similar to the present data, a recent study demonstrates that stimulation of NMDA receptors drives the shrinkage of dendritic spines via the cofilin-dependent severing of the actin cytoskeleton in the hippocampal CA1 neurons [59]. Taken together, these findings suggest that repeated nicotine exposure increases the membrane expression of the GluN2B subunits in dendrites followed by the receptor-coupled activation of LIMK1, leading to the elevation of actin turnover in a cofilin-dependent manner in MSN of the CPu.

The dynamic changes in F-actin filaments are mediated by the stimulation of GluN2B subunits, through which cofilin is closely linked to the structural flexibility and adaptive changes [3, 4, 47, 60, 61]. Viral overexpression of active cofilin mimics the cocaine-induced increase in the thin spines of MSN in the NAc, potentiating the cocaine-induced conditioned place preference [22]. The previous study has also demonstrated that an increase in both actin cycling and the spine diameter in the NAc influences the challenge cocaine-induced locomotor sensitization [25]. Similarly, the present study shows a potential linkage between the repeated nicotine-induced shrinkage of the spine head and the development of behavioral sensitization. Therefore, these findings suggest that morphological changes in the dendritic spines mediated by cofilin have been implicated in the long-term changes of the glutamate synapses in the CPu, which appears to drive habitual behaviors after chronic exposure to nicotine.

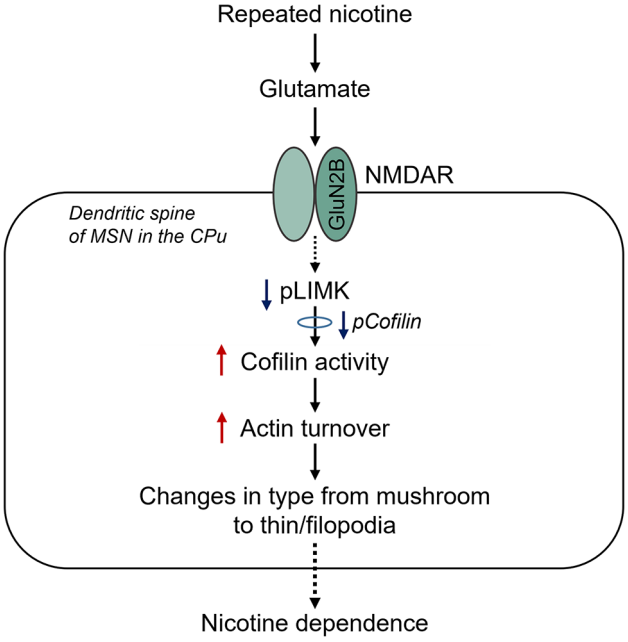

Fig. 7 A diagram illustrating the nicotine-induced spine remodeling via GluN2B subunits-linked cofilin activity in the MSN. The elevation of glutamate release after repeated nicotine exposure leads to a reduction of pLIMK and subsequent pCofilin, which enables the active state of cofilin from its inactive state. Activation of cofilin in turn drives spine shrinkage from mushroom spines into thin spines/filopodia by increasing actin turnover

Conclusions

As depicted in Fig. 7, stimulation of GluN2B subunits of NMDA receptors after repeated nicotine exposure activates cofilin by reducing its phosphorylation state probably via LIMK1 inhibition. Activated cofilin seems to shift the formation of more thin spines/filopodia from mushroom types of spines by potentiating actin turnover. The cofilin-mediated decreases in head diameter and the transition from mushroom to thin spines/filopodia simultaneously affect the development of locomotor sensitization. The novel findings presented in the present study may provide insight into the understanding of nicotine dependence that underlies synaptic remodeling by disturbing the glutamatergic synapses in the CPu after chronic exposure to nicotine in rats.

Acknowledgements

Not applicable.

Author contributions

SK and ESC contributed to the study conception and design. Experiments, data collection and statistical analysis were performed by SK and SS. The first draft of the manuscript was written by SK and all authors commented on previous versions of the manuscript. ESC supervised the study and edited the manuscript. All authors read and approved the final manuscript.

Funding

This work was supported by a grant from the National Research Foundation of Korea (2021R1A2C2008083 to E.S.C.).

Data availability
No datasets were generated or analysed during the current study.

Declarations

Ethics approval and consent to participate
The animal protocol used in this study has been reviewed by the Pusan National University-Institutional Animal Care and Use Committee (PNU-IACUC) on their ethical procedures and scientific care, and it has been approved (Busan, Korea, Az.: PNU-2022-3169; PNU-2023-3236).

Consent for publication
Not applicable.

Competing interests
The authors declare no competing interests.

Received: 17 June 2024 / Accepted: 30 September 2024
Published online: 14 October 2024

References

1. Stolerman IP, Jarvis MJ. The scientific case that nicotine is addictive. Psychopharmacology. 1995;117:2–20. https://doi.org/10.1007/BF02245088.
2. Le Foll B, Goldberg SR. Nicotine as a typical drug of abuse in experimental animals and humans. Psychopharmacology. 2006;184:367–81. https://doi.org/10.1007/s00213-005-0155-8.
3. D'Souza MS, Markou A. Neuronal mechanisms underlying development of nicotine dependence: implications for novel smoking-cessation treatments. Addict Sci Clin Pract. 2011;6(1):4–16.
4. Robinson TE, Kolb B. Structural plasticity associated with exposure to drugs of abuse. Neuropharmacology. 2004;47(Suppl 1):33–46. https://doi.org/10.1016/j.neuropharm.2004.06.025.
5. Jones S, Bonci A. Synaptic plasticity and drug addiction. Curr Opin Pharmacol. 2005;5(1):20–5. https://doi.org/10.1016/j.coph.2004.08.011.
6. Hyman SE, Malenka RC, Nestler EJ. Neural mechanisms of addiction: the role of reward-related learning and memory. Annu Rev Neurosci. 2006;29:565–98. https://doi.org/10.1146/annurev.neuro.29.051605.113009.
7. Kauer JA, Malenka RC. Synaptic plasticity and addiction. Nat Rev Neurosci. 2007;8(11):844–58. https://doi.org/10.1038/nrn2234.
8. Russo SJ, Dietz DM, Dumitriu D, Morrison JH, Malenka RC, Nestler EJ. The addicted synapse: mechanisms of synaptic and structural plasticity in nucleus accumbens. Trends Neurosci. 2010;33(6):267–76. https://doi.org/10.1016/j.tins.2010.02.002.
9. Dani JA, De Biasi M. Cellular mechanisms of nicotine addiction. Pharmacol Biochem Behav. 2001;70(4):439–46. https://doi.org/10.1016/s0091-3057(01)00652-9.
10. Yin HH, Knowlton BJ. The role of the basal ganglia in habit formation. Nat Rev Neurosci. 2006;7:464–76. https://doi.org/10.1038/nrn1919.
11. Changeux JP. Nicotine addiction and nicotinic receptors: lessons from genetically modified mice. Nat Rev Neurosci. 2010;11:389–401. https://doi.org/10.1038/nrn2849.
12. Ryu IS, Kim J, Seo SY, Yang JH, Oh JH, Lee DK, Cho HW, Yoon SS, Seo JW, Chang S, Kim HY, Shim I, Choe ES. Behavioral changes after nicotine challenge are associated with α7 nicotinic acetylcholine receptor-stimulated glutamate release in the rat dorsal striatum. Sci Rep. 2017;7:15009. https://doi.org/10.1038/s41598-017-15161-7.
13. Kim S, Sohn S, Ryu IS, Yang JH, Kim OH, Kim JS, Kim YH, Jang EY, Choe ES. Nicotine Rather Than Non-nicotine substances in 3R4F WCSC increases behavioral sensitization and drug-taking behavior in rats. Nicotine Tob Res. 2022;24(8):1201–7. https://doi.org/10.1093/ntr/ntac063.
14. Schwabe L, Dickinson A, Wolf OT. Stress, habits, and drug addiction: a psychoneuroendocrinological perspective. Exp Clin Psychopharmacol. 2011;19(1):53–63. https://doi.org/10.1037/a0022212.
15. Adermark L, Morud J, Lotfi A, Danielsson K, Ulenius L, Söderpalm B, Ericson M. Temporal rewiring of Striatal Circuits initiated by Nicotine. Neuropsychopharmacology. 2016;41(13):3051–9. https://doi.org/10.1038/npp.2016.118.
16. Ehlinger DG, Burke JC, McDonald CG, Smith RF, Bergstrom HC. Nicotine-induced and D1-receptor-dependent dendritic remodeling in a subset of dorsolateral striatum medium spiny neurons. Neuroscience. 2017;356:242–54. https://doi.org/10.1016/j.neuroscience.2017.05.036.
17. Xia J, Meyers AM, Beeler JA. Chronic nicotine alters corticostriatal plasticity in the Striatopallidal pathway mediated by NR2B-Containing Silent synapses. Neuropsychopharmacology. 2017;42(12):2314–24. https://doi.org/10.1038/npp.2017.87.
18. Carlier MF, Laurent V, Santolini J, Melki R, Didry D, Xia GX, Hong Y, Chua NH, Pantaloni D. Actin depolymerizing factor (ADF/cofilin) enhances the rate of filament turnover: implication in actin-based motility. J Cell Biol. 1997;136(6):1307–22. https://doi.org/10.1083/jcb.136.6.1307.
19. Bamburg JR. Proteins of the ADF/cofilin family: essential regulators of actin dynamics. Annu Rev Cell Dev Biol. 1999;15:185–230. https://doi.org/10.1146/annurev.cellbio.15.1.185.
20. Racz B, Weinberg RJ. Spatial organization of cofilin in dendritic spines. Neuroscience. 2006;138(2):447–56. https://doi.org/10.1016/j.neuroscience.2005.11.025.
21. Lappalainen P, Drubin DG. (1997) Cofilin promotes rapid actin filament turnover in vivo. Nature. 1997;388(6637):78–82. https://doi.org/10.1038/40418
22. Dietz DM, Sun H, Lobo MK, Cahill ME, Chadwick B, Gao V, Koo JW, Mazei-Robison MS, Dias C, Maze I, Damez-Werno D, Dietz KC, Scobie KN, Ferguson D, Christoffel D, Ohnishi Y, Hodes GE, Zheng Y, Neve RL, Hahn KM, Russo SJ, Nestler EJ. Rac1 is essential in cocaine-induced structural plasticity of nucleus accumbens neurons. Nat Neurosci. 2012;15(6):891–6. https://doi.org/10.1038/nn.3094.
23. Kruyer A, Ball LE, Townsend DM, Kalivas PW, Uys JD. Post-translational S-glutathionylation of cofilin increases actin cycling during cocaine seeking. PLoS ONE. 2019;14(9):e0223037. https://doi.org/10.1371/journal.pone.0223037.
24. Rigoni D, Avalos MP, Boezio MJ, Guzmán AS, Calfa GD, Perassi EM, Pierotti SM, Bisbal M, Garcia-Keller C, Cancela LM, Bollati F. Stress-induced vulnerability to develop cocaine addiction depends on cofilin modulation. Neurobiol Stress. 2021;15:100349. https://doi.org/10.1016/j.ynstr.2021.100349.
25. Toda S, Shen H, Kalivas PW. Inhibition of actin polymerization prevents cocaine-induced changes in spine morphology in the nucleus accumbens. Neurotox Res. 2010;18:410–5. https://doi.org/10.1007/s12640-010-9193-z.
26. Shoji K, Ohashi K, Sampei K, Oikawa M, Mizuno K. Cytochalasin D acts as an inhibitor of the actin-cofilin interaction. Biochem Biophys Res Commun. 2012;424(1):52–7. https://doi.org/10.1016/j.bbrc.2012.06.063.
27. Mantzur L, Joels G, Lamprecht R. Actin polymerization in lateral amygdala is essential for fear memory formation. Neurobiol Learn Mem. 2009;91(1):85–8. https://doi.org/10.1016/j.nlm.2008.09.001.
28. Go BS, Barry SM, McGinty JF. Glutamatergic neurotransmission in the prefrontal cortex mediates the suppressive effect of intra-prelimbic cortical infusion of BDNF on cocaine-seeking. Eur Neuropsychopharmacol. 2016;26(12):1989–99. https://doi.org/10.1016/j.euroneuro.2016.10.002.
29. Choe ES, Parelkar NK, Kim JY, Cho HW, Kang HS, Mao L, Wang JQ. The protein phosphatase 1/2A inhibitor okadaic acid increases CREB and Elk-1 phosphorylation and c-fos expression in the rat striatum in vivo. J Neurochem. 2004;89:383–90. https://doi.org/10.1111/j.1471-4159.2003.02334.x.
30. Schindelin J, Arganda-Carreras I, Frise E, Kaynig V, Longair M, Pietzsch T, Preibisch S, Rueden C, Saalfeld S, Schmid B, Tinevez JY, White DJ, Hartenstein V, Eliceiri K, Tomancak P, Cardona A. Fiji: an open-source platform for biological-image analysis. Nat Methods. 2012;9:676–82. https://doi.org/10.1038/nmeth.2019.
31. Baker GE, Reese BE. Using confocal laser scanning microscopy to investigate the organization and development of neuronal projections labeled with DiI. Methods Cell Biol. 1993;38:325–44. https://doi.org/10.1016/s0091-679x(08)61009-2.
32. Wang J, Li KL, Shukla A, Beroun A, Ishikawa M, Huang X, Wang Y, Wang YQ, Bastola ND, Huang HH, Kramer LE, Chao T, Huang YH, Sesack SR, Nestler EJ, Schlüter OM, Dong Y. Cocaine Triggers Glial-Mediated Synaptogenesis. bioRxiv. 2020. https://doi.org/10.1101/2020.01.20.896233
33. Wright WJ, Graziane NM, Neumann PA, Hamilton PJ, Cates HM, Fuerst L, Spenceley A, MacKinnon-Booth N, Iyer K, Huang YH, Shaham Y, Schlüter OM, Nestler EJ, Dong Y. Silent synapses dictate cocaine memory destabilization and reconsolidation. Nat Neurosci. 2020;23(1):32–46. https://doi.org/10.1038/s41593-019-537-6.
34. Wang YQ, Wang J, Xia SH, Gutstein HB, Huang YH, Schlüter OM, Cao JL, Dong Y. Neuropathic pain generates silent synapses in thalamic projection to anterior cingulate cortex. Pain. 2021;162(5):1322–33. https://doi.org/10.1097/j.pain.0000000000002149.
35. Boudreau AC, Milovanovic M, Conrad KL, Nelson C, Ferrario CR, Wolf ME. A protein cross-linking assay for measuring cell surface expression

of glutamate receptor subunits in the rodent brain after in vivo treatments. Curr Protoc Neurosci Apr. 2012;Chap. 5:Unit 5.30.1–19. https://doi.org/10.1002/0471142301.ns0530s59
36. Ryu IS, Kim J, Seo SY, Yang JH, Oh JH, Lee DK, Cho HW, Lee K, Yoon SS, Seo JW, Shim I, Choe ES. Repeated Administration of Cigarette Smoke Condensate increases glutamate levels and behavioral sensitization. Front Behav Neurosci. 2018;12:47. https://doi.org/10.3389/fnbeh.2018.00047.
37. Dumitriu D, Rodriguez A, Morrison JH. High-throughput, detailed, cell-specific neuroanatomy of dendritic spines using microinjection and confocal microscopy. Nat Protoc. 2011;6(9):1391–411. https://doi.org/10.1038/nprot.2011.389.
38. Pröschel C, Blouin MJ, Gutowski NJ, Ludwig R, Noble M. Limk1 is predominantly expressed in neural tissues and phosphorylates serine, threonine and tyrosine residues in vitro. Oncogene. 1995;11:1271–81.
39. Kim S, Sohn S, Choe ES. Phosphorylation of GluA1-Ser831 by CaMKII activation in the Caudate and Putamen is required for behavioral sensitization after challenge nicotine in rats. Int J Neuropsychopharmacol. 2022;25(8):678–87. https://doi.org/10.1093/ijnp/pyac034.
40. Graziane NM, Sun S, Wright WJ, Jang D, Liu Z, Huang YH, Nestler EJ, Wang YT, Schlüter OM, Dong Y. Opposing mechanisms mediate morphine- and cocaine-induced generation of silent synapses. Nat Neurosci. 2016;19(7):915–25. https://doi.org/10.1038/nn.4313.
41. Hotulainen P, Llano O, Smirnov S, Tanhuanpää K, Faix J, Rivera C, Lappalainen P. Defining mechanisms of actin polymerization and depolymerization during dendritic spine morphogenesis. J Cell Biol. 2009;185(2):323–39. https://doi.org/10.1083/jcb.200809046.
42. Shi Y, Pontrello CG, DeFea KA, Reichardt LF, Ethell IM. Focal adhesion kinase acts downstream of EphB receptors to maintain mature dendritic spines by regulating cofilin activity. J Neurosci. 2009;29(25):8129–42. https://doi.org/10.1523/JNEUROSCI.4681-08.2009.
43. Yang N, Higuchi O, Ohashi K, Nagata K, Wada A, Kangawa K, Nishida E, Mizuno K. Cofilin phosphorylation by LIM-kinase 1 and its role in rac-mediated actin reorganization. Nature. 1998;393(6687):809–12. https://doi.org/10.1038/31735.
44. Arber S, Barbayannis FA, Hanser H, Schneider C, Stanyon CA, Bernard O, Caroni P. Regulation of actin dynamics through phosphorylation of cofilin by LIM-kinase. Nature. 1998;393(6687):805–9. https://doi.org/10.1038/31729.
45. Meng Y, Takahashi H, Meng J, Zhang Y, Lu G, Asrar S, Nakamura T, Jia Z. Regulation of ADF/cofilin phosphorylation and synaptic function by LIM-kinase. Neuropharmacology. 2004;47(5):746–54. https://doi.org/10.1016/j.neuropharm.2004.06.030.
46. Toda S, Shen HW, Peters J, Cagle S, Kalivas PW. Cocaine increases actin cycling: effects in the reinstatement model of drug seeking. J Neurosci. 2006;26(5):1579–87. https://doi.org/10.1523/JNEUROSCI.4132-05.2006.
47. Shen HW, Toda S, Moussawi K, Bouknight A, Zahm DS, Kalivas PW. Altered dendritic spine plasticity in cocaine-withdrawn rats. J Neurosci. 2009;29(9):2876–84. https://doi.org/10.1523/JNEUROSCI.5638-08.2009.
48. Robinson TE, Kolb B. Alterations in the morphology of dendrites and dendritic spines in the nucleus accumbens and prefrontal cortex following repeated treatment with amphetamine or cocaine. Eur J Neurosci. 1999;11(5):1598–604. https://doi.org/10.1046/j.1460-9568.1999.00576.x.
49. Xia SH, Yu J, Huang X, Sesack SR, Huang YH, Schlüter OM, Cao JL, Dong Y. Cortical and thalamic Interaction with Amygdala-to-Accumbens synapses. J Neurosci. 2020;40(37):7119–32. https://doi.org/10.1523/JNEUROSCI.1121-20.2020.
50. Robinson TE, Gorny G, Mitton E, Kolb B. Cocaine self-administration alters the morphology of dendrites and dendritic spines in the nucleus accumbens and neocortex. Synapse. 2001;39(3):257–66. https://doi.org/10.1002/1098-2396(20010301)39:3257::AID-SYN10073.0.CO;2-1.
51. Brown RW, Kolb B. Nicotine sensitization increases dendritic length and spine density in the nucleus accumbens and cingulate cortex. Brain Res. 2001;899(1–2):94–100. https://doi.org/10.1016/s0006-8993(01)02201-6.
52. Brown TE, Lee BR, Mu P, Ferguson D, Dietz D, Ohnishi YN, Lin Y, Suska A, Ishikawa M, Huang YH, Shen H, Kalivas PW, Sorg BA, Zukin RS, Nestler EJ, Dong Y, Schlüter OM. A silent synapse-based mechanism for cocaine-induced locomotor sensitization. J Neurosci. 2011;31(22):8163–74. https://doi.org/10.1523/JNEUROSCI.0016-11.2011.
53. Robinson TE, Kolb B. Persistent structural modifications in nucleus accumbens and prefrontal cortex neurons produced by previous experience with amphetamine. J Neurosci. 1997;17(21):8491–7. https://doi.org/10.1523/JNEUROSCI.17-21-08491.1997.
54. Peters A, Kaiserman-Abramof IR. The small pyramidal neuron of the rat cerebral cortex. The perikaryon, dendrites and spines. Am J Anat. 1970;127(4):321–55. https://doi.org/10.1002/aja.1001270402.
55. Arellano JI, Benavides-Piccione R, Defelipe J, Yuste R. Ultrastructure of dendritic spines: correlation between synaptic and spine morphologies. Front Neurosci. 2007;1(1):131–43. https://doi.org/10.3389/neuro.01.1.1.010.2007.
56. Ofer N, Berger DR, Kasthuri N, Lichtman JW, Yuste R. Ultrastructural analysis of dendritic spine necks reveals a continuum of spine morphologies. Dev Neurobiol. 2021;81(5):746–57. https://doi.org/10.1002/dneu.22829.
57. Huang YH, Lin Y, Mu P, Lee BR, Brown TE, Wayman G, Marie H, Liu W, Yan Z, Sorg BA, Schlüter OM, Zukin RS, Dong Y. In vivo cocaine experience generates silent synapses. Neuron. 2009;63(1):40–7. https://doi.org/10.1016/j.neuron.2009.06.007.
58. Leyrer-Jackson JM, Piña JA, McCallum J, Foster Olive M, Gipson CD. Direct administration of ifenprodil and citalopram into the nucleus accumbens inhibits cue-induced nicotine seeking and associated glutamatergic plasticity. Brain Struct Funct. 2020;225(7):1967–78. https://doi.org/10.1007/s00429-020-02103-9.
59. Stein IS, Park DK, Flores JC, Jahncke JN, Zito K. Molecular mechanisms of non-ionotropic NMDA receptor signaling in dendritic spine shrinkage. J Neurosci. 2020;40(19):3741–50. https://doi.org/10.1523/JNEUROSCI.0046-20.2020.
60. Garcia-Keller C, Scofield MD, Neuhofer D, Varanasi S, Reeves MT, Hughes B, Anderson E, Richie CT, Mejias-Aponte C, Pickel J, Hope BT, Harvey BK, Cowan CW, Kalivas PW. Relapse-Associated transient synaptic potentiation requires integrin-mediated activation of focal adhesion kinase and Cofilin in D1-Expressing neurons. J Neurosci. 2020;40(44):8463–77. https://doi.org/10.1523/JNEUROSCI.2666-19.2020.
61. Kalivas PW. The glutamate homeostasis hypothesis of addiction. Nat Rev Neurosci. 2009;10(8):561–72. https://doi.org/10.1038/nrn2515.

Publisher's note